J Mater Sci (2010) 45:5685–5691
DOI 10.1007/s10853-010-4634-x

Template-free hydrothermal synthesis of hollow hematite microspheres

Qiang Dong · Nobuhiro Kumada · Yoshinori Yonesaki · Takahiro Takei · Nobukazu Kinomura · Dan Wang

Received: 29 January 2010 / Accepted: 18 May 2010 / Published online: 5 June 2010

Abstract Hollow hematite (α-Fe_2O_3) microspheres with an average diameter of 3-4 μm and a shell thickness of approximate 150 nm was synthesized by a simple hydrothermal route using $FeCl_3 \cdot 6H_2O$ solution and acetic acid without using any templates. The hollow microspheres were composed of α-Fe_2O_3 nanoparticles with the diameter range from 20 to 40 nm. The effects of reaction parameters such as reaction time, temperature, concentration of $FeCl_3 \cdot 6H_2O$ solution, and initial pH on the morphology of the final products were investigated. A possible formation mechanism of hollow α-Fe_2O_3 microspheres was also proposed, where the acetic acid played a role of etching in the formation of hollow structure.

Introduction

In recent years, the preparation of nanometer and micrometer materials with desired morphologies has attracted increasing interest due to their various shape-induced functions. Among these materials, hollow spheres with nanometer-to-micrometer dimensions are of much interest because of their many potential applications, including controlled release capsules for various substances, artificial cells, catalysts, fillers, battery materials, pigments, coatings, drug delivery carriers, and lightweight structural materials [1–10]. Many synthetic approaches have been developed for hollow spheres, including metals and oxides. Many of them are based on hard templates, such as silica spheres [11, 12], polymer latex colloids [7, 13], and carbon spheres [14], or soft templates, such as gas bubbles [15, 16], emulsion droplets [17, 18], and surfactant vesicles [19]. The template-directed approaches are effective for controlling the morphology of the final products. However, using a template may complicate the synthetic procedure and limit the scale at which a product can be processed each time. Additionally, the introduction of impurities into the product is usually inevitable with template methods and removing the impurities is usually time-consuming. Consequently, more attention has been focused on template-free synthesis methods for hollow spheres.

Iron oxides, which have many practical applications in pigments, catalysis, and magnetic recording materials, constitute a very important family in material science [20]. In this family, hematite (α-Fe_2O_3), an environmentally friendly n-type semiconductor with a band gap of 2.2 eV, is widely used in catalysts, pigments, sensors, and as the raw material for the synthesis of magnetic γ-Fe_2O_3, which is of great importance as a ferrofluid and magnetic recording material [20–24]. In addition to the conventional applications of hematite in these fields, hollow hematite spheres perform remarkably in photocatalysis, water treatment, and lithium ion batteries [25–29], and much attention has been paid to their synthesis. For example, Zhang et al. [30] synthesized uniform polystyrene/α-Fe_2O_3 composite hollow microspheres. Hollow spheres of α-Fe_2O_3 varying size in from 100 to 400 nm were prepared using carbonaceous spheres as templates [31].

Q. Dong · N. Kumada (✉) · Y. Yonesaki · T. Takei · N. Kinomura
Department of Research Interdisciplinary Graduate School of Medicine and Engineering, University of Yamanashi, Miyamae cho-7, Kofu 400-8511, Japan
e-mail: kumada@yamanashi.ac.jp

D. Wang
State Key Laboratory of Multi-Phase & Complex Systems, Institute of Process Engineering, Chinese Academy of Sciences, Beijing 100080, China

Submicrometer-sized hollow hematite particles have been prepared using a surfactant-assisted solvothermal process [26]. A template-free approach has been used to synthesize novel hollow α-Fe_2O_3 spheres in the presence of the surfactant CTAB [27]. Cao et al. [28, 29] fabricated α-Fe_2O_3 hierarchically nanostructured hollow spheres using a two-step surfactant-free solvothermal method. However, most of the existing methods for synthesizing hollow hematite spheres involve templates, surfactants, toxic organic solvents, or complicated operations; additionally, the starting materials are relatively complex and expensive. Thus, exploring simple, low-cost methods for synthesizing hollow hematite spheres is of great interest for their large-scale application in catalysts and encapsulation.

Our group has successfully prepared α-Fe_2O_3 and Fe_3O_4 in various shapes using simple hydrothermal methods [32, 33]. We also found that hollow Fe_3O_4 spheres could be prepared via a template-free hydrothermal reaction [34]. Here, we introduce a fast, template-free hydrothermal method for synthesizing hollow α-Fe_2O_3 microspheres with no additives. Due to its simplicity, this process can be readily reproduced and scaled-up, which should facilitate the preparation and application of hollow hematite microspheres.

Experimental section

Preparation of hollow α-Fe_2O_3 microspheres

Acetic acid (CH_3COOH), 0–3 mL (6 mol dm^{-3}), was added to 22 mL $FeCl_3{\cdot}6H_2O$ solution (1 mol dm^{-3}) for adjusting the initial pH at room temperature. Then, the mixture was put into a 50 mL Teflon-lined autoclave. The autoclave was sealed, and maintained at 160 °C for 20 h, and then cooled to room temperature naturally. After centrifugation, the products were obtained and washed with distilled water and absolute ethanol two times, respectively, finally dried in air at 60 °C for 6 h.

Characterization

X-ray powder diffraction (XRD) was performed on a Rigaku X-ray diffractometer (RINT2000V Japan) with graphite-monochromatized CuKα radiation ($\lambda = 1.54056$ Å) using 30 mA and 40 kV. The diffraction pattern over the range of 10–70° in 2θ was recorded with a scanning speed of 3° min^{-1}. Scanning electron microscopy (SEM) images were taken with a JEOL JEM-6500F field emission scanning electron microscope. Transmission electron microscopy (TEM) images were taken with a JEOL JEM-2000FXII transmission electron microscope using an accelerating voltage of 200 kV. The samples used for TEM observations were prepared by dispersing products in ethanol under ultrasonic agitation for 10 min, then placing a drop of the dispersion onto a copper grid coated with a layer of amorphous carbon. Fourier transform infrared (FT-IR) spectra were recorded in the range of 4000–400 cm^{-1} on a JASCO FT/IR-4100 spectrometer by using KBr pellets. Thermogravimetric analysis (TGA) and mass spectrometry of gas species were carried out in a Rigaku Thermo Plus TG 8120 thermal analysis system with a heating rate of 10 °C min^{-1} from room temperature to 800 °C under a flow of helium.

Results and discussion

Synthesis of hollow α-Fe_2O_3 microspheres

Figure 1d shows a typical X-ray diffraction (XRD) pattern of the products produced at 160 °C at an initial pH of 0.9 after reacting for 20 h. All peaks in the XRD pattern can be indexed as α-Fe_2O_3 (JCPDS 33-664) and no impurity phase is observed. The product consisted of hollow α-Fe_2O_3 microspheres with diameters of 3–4 μm and shells approximately 150 nm thickness (Fig. 2a–c). The high magnification image (Fig. 2c) shows that the hollow α-Fe_2O_3 microspheres are an aggregation of nanoparticles with diameters of 20–40 nm. And the hematite microspheres with hollow structures were also confirmed by the TEM observation (Fig. 2d).

Effect of reaction time

The time-dependent evolution of the morphology at 160 °C is shown in Fig. 3. At a short reaction time of 1 h, urchin-like particles were obtained, which were assembled from

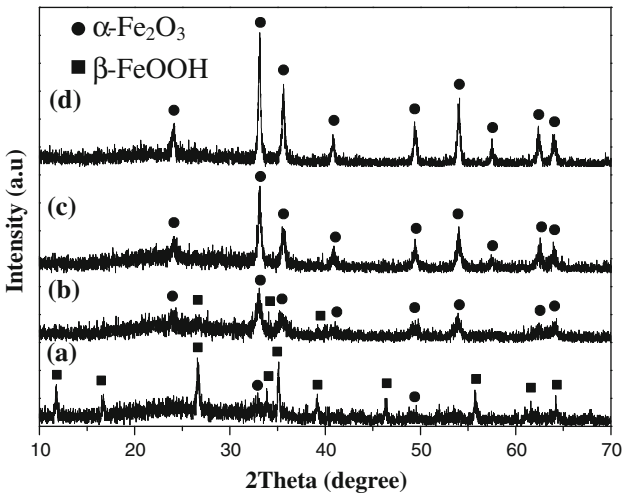

Fig. 1 X-ray powder diffraction patterns of the products produced at 160 °C under the initial pH of 0.9. (*a*) 1 h, (*b*) 2 h, (*c*) 5 h, (*d*) 20 h

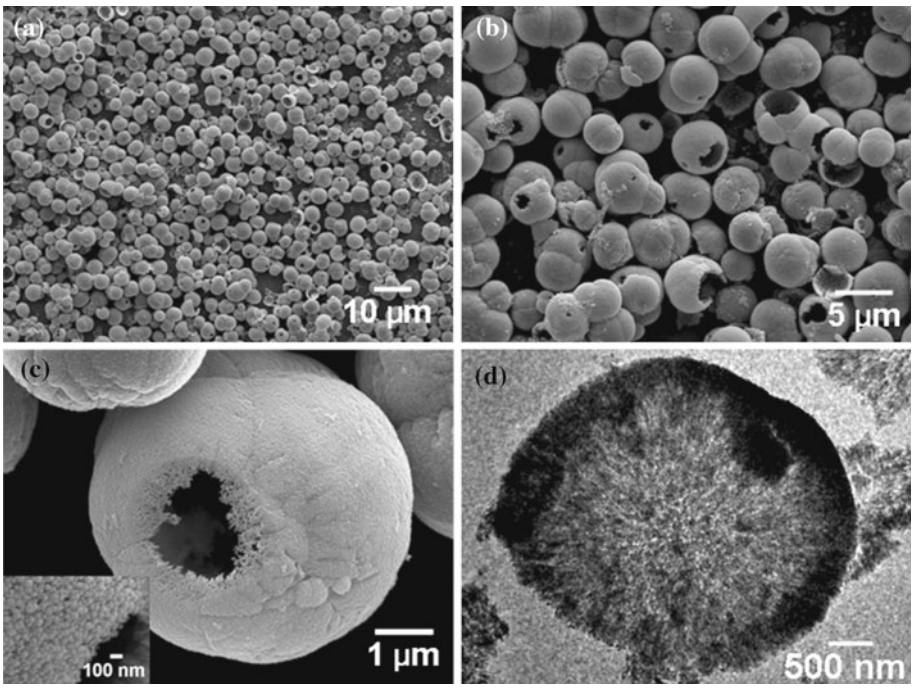

Fig. 2 SEM and TEM images of the hematite particles produced at 160 °C for 20 h under the initial pH of 0.9

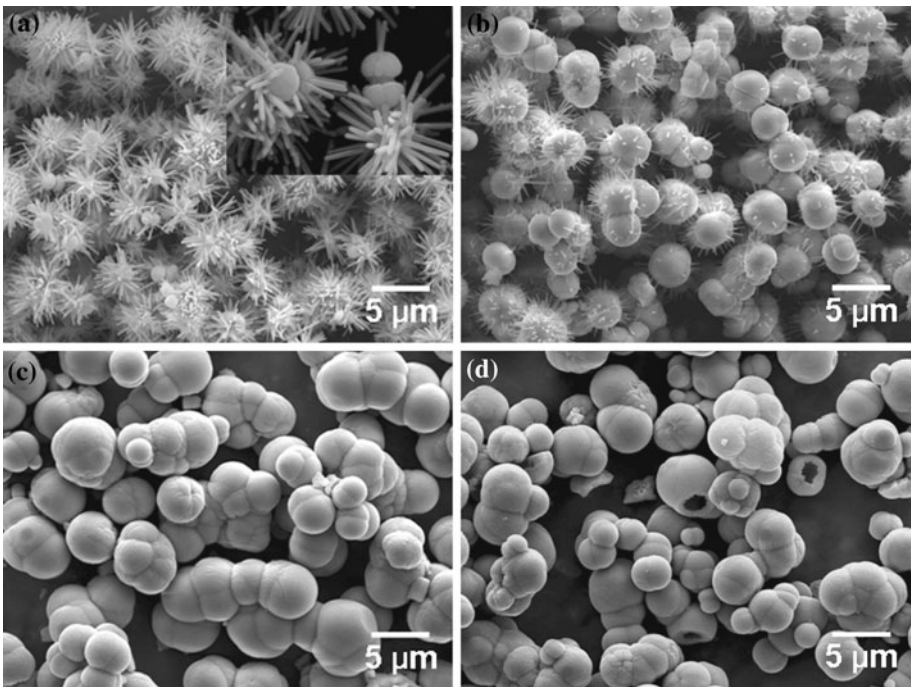

Fig. 3 SEM images of the hematite particles produced at different reaction time at 160 °C under the initial pH of 0.9. **a** 1 h, **b** 2 h, **c** 5 h, **d** 9 h

nanorods with diameters in the range 100–150 nm and lengths of 1.5–2.0 μm (Fig. 3a). These urchin-like particles were identified as akaganeite (β-FeOOH) by XRD (Fig. 1a). Additionally, a few spherical hematite particles were observed around the urchin-like particles. After 2 h of the hydrothermal process, some particles with new morphologies appeared (Fig. 3b); these were spheres with diameters of 3–4 μm and nanorods could be observed on the surfaces of the spherical hematite particles, indicating that the akaganeite had been transformed into hematite over time. XRD results showed that the products were a mixture of akaganeite and hematite (Fig. 1b). When the reaction time exceeded 5 h, large-volume microspheres predominated in the product (Fig. 3c), and the microspheres were identified as hematite by XRD (Fig. 1c). As the reaction time was prolonged to 9 h, hollow microspheres formed (Fig. 3d). The uniform hollow microspheres replaced all of the urchin-like akaganeite as the

reaction time was extended to 20 h (Fig. 2a). However, at reaction times exceeding 40 h, no product was obtained.

Effect of reaction temperature

In our experiments, the products obtained at a reaction temperature below 160 °C were mainly spherical particles (140 °C, Fig. 4b) or irregular particles (120 °C, Fig. 4a). Only when the reaction temperature was at 160 °C, uniform hollow microspheres could be formed (160 °C, Fig. 2a). As the temperature was above 180 °C, no precipitation was obtained.

Effect of the concentration of the $FeCl_3 \cdot 6H_2O$ solution

The concentration of the $FeCl_3 \cdot 6H_2O$ solution was also found to be important for the formation of uniform, regular hollow α-Fe_2O_3 microspheres. Keeping the volume of CH_3COOH constant at 2 mL, a low concentration (0.025 mol dm^{-3}) of $FeCl_3 \cdot 6H_2O$ solution resulted in the formation of spherical particles with a size of 100 nm, composed of nanoparticles (Fig. 5a), at a slightly higher concentration (0.0625 mol dm^{-3}), spherical particles with a size of 500 nm could be obtained (Fig. 5b), and the size of the hollow microspheres increased gradually, from 2 to 4 μm, as the concentration of $FeCl_3 \cdot 6H_2O$ solution increased, from 0.25 to 0.5 mol dm^{-3} (Fig. 5c, d). Uniform hollow α-Fe_2O_3 microspheres were observed as the concentration increased to 1 mol dm^{-3}. However, no product was obtained at concentrations higher than 1.5 mol dm^{-3}. Additionally, at 0.025 mol dm^{-3}, the initial pH was 1.8, and the initial pH decreased as the concentration increased; it was 1.6, 1.3, 1.1, 0.9, and 0.5 at concentrations of 0.0625, 0.25, 0.5, 1.0, and 1.5 mol dm^{-3}, respectively. Our experiments suggested that the appropriate concentration range was from 0.25 to 1 mol dm^{-3}.

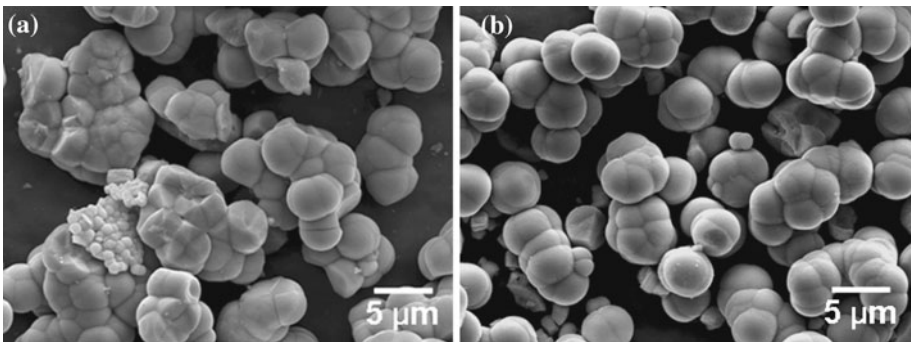

Fig. 4 SEM images of the hematite particles produced at different reaction temperatures for 24 h under the initial pH of 0.9. **a** 120 °C, **b** 140 °C

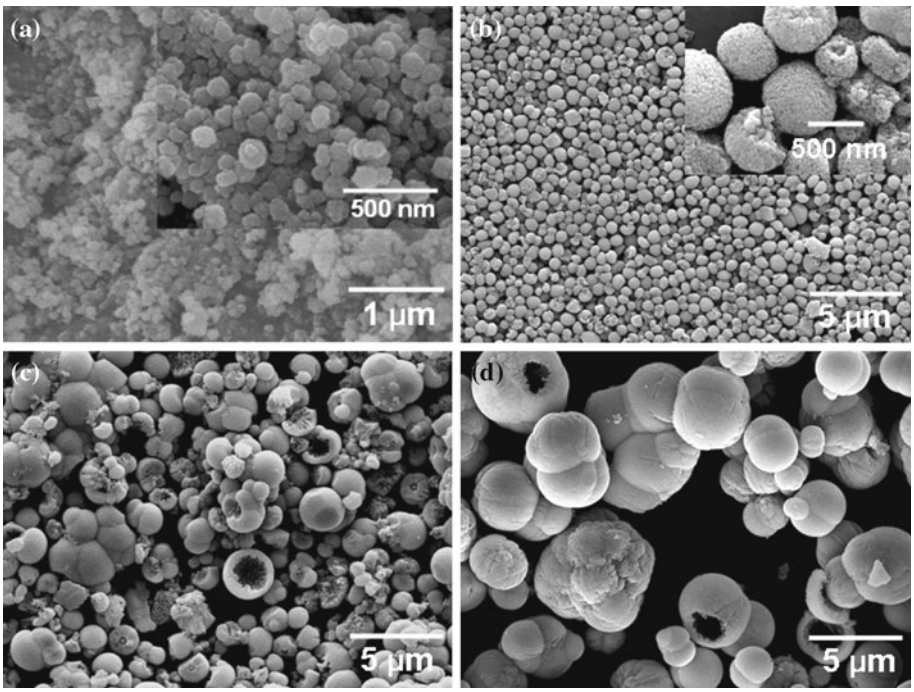

Fig. 5 SEM images of the hematite particles produced at 120 °C for 24 h with different concentrations of $FeCl_3 \cdot 6H_2O$ solutions. **a** 0.025 mol dm^{-3}, **b** 0.0625 mol dm^{-3}, **c** 0.25 mol dm^{-3}, **d** 0.5 mol dm^{-3}

Effect of initial pH

The initial pH was controlled to test its effect on the morphology of the products by systematically altering the volume of acetic acid. At an initial pH of 1.4 (no acetic acid), hematite particles were formed (Fig. 6a). Most of the particles had diameters of 3–4 μm. Decreasing the initial pH to 1.1 (0.8 mL acetic acid) led to the formation of a few hollow α-Fe_2O_3 microspheres (Fig. 6b). When the initial pH was decreased to 0.9 (2 mL of acetic acid), the volume of the hollow α-Fe_2O_3 microspheres increased and the thickness of the shell decreased (Fig. 2b). No hollow α-Fe_2O_3 microspheres were observed when the initial pH was 0.7 (3 mL of acetic acid; Fig. 6c), and few integral particles were found, due to the decreased shell thickness in the strongly acidic conditions. When the initial pH was lower than 0.7, no precipitate was obtained, indicating that hematite particles could not form in such an environment. From these results, hollow α-Fe_2O_3 microspheres were obtained at an initial pH of 1.1–0.7 (0.8–3 mL of acetic acid), and the initial pH may play an important role in the formation of hollow α-Fe_2O_3 microspheres.

Formation mechanism of hollow hematite microspheres

In this work, hollow hematite microspheres were obtained by carefully controlling reaction parameters. The formation of the hollow hematite microspheres can be described as follows. First, urchin-like akaganeite (Fig. 3a) forms quickly as a result of the hydrolysis of Fe^{3+} under hydrothermal conditions. The formation of the urchin-like akaganeite is probably due to the radial growth of akaganeite nanorods on the spherical akaganeite nuclei [35]. Then, after sufficiently long reaction times, a dissolution–recrystallization process occurs, transforming the akaganeite into hematite, which tends to crystallize on the surface of the undissolved urchin-like akaganeite to minimize the surface energy. The hematite nanoparticles between the nanorods of the urchin-like akaganeite that emerges at a reaction time of 1 h are the result of the nucleation and initial growth of hematite. As the reaction proceeds to 2 h, the hematite particles grow bigger and join together to form spherical hematite particles (Fig. 3b). When the reaction time is extended to 5 h, the hematite microspheres form (Fig. 3c). Etching or the partial dissolution of the interior of particles using acid is one approach for synthesizing hollow or porous materials [36]. GaN hollow spheres were produced by removing gallium cores in aqua regia [37]. Hollow α-Fe_2O_3 nanoboxes were synthesized when α-Fe_2O_3 nanocubes were used as a starting material, and alkylphosphonic acid was responsible for the etching process [38].

Recently, etching copper oxide using acetic acid was investigated [39]. Here, hollow α-Fe_2O_3 microspheres are formed as the reaction time is prolonged to 20 h (2 mL acetic acid; Fig. 2), and the formation of hollow α-Fe_2O_3 microspheres is thought to have been caused by chemical etching due to the use of a weak acid (acetic acid). In this reaction system, the acetic acid etching of the hematite microspheres proceeds and the hematite hollow microspheres form as a result. In this process, hematite reacts with acetic acid to produce $Fe(CH_3COO)_3$. In the case of a slightly higher initial pH of 1.1 (0.8 mL acetic acid; Fig. 6b), only a few hollow α-Fe_2O_3 microspheres form, which are partially etched. However, no hollow α-Fe_2O_3 microspheres are observed and few integral particles obtained at a low initial pH of 0.7 (3 mL of acetic acid; Fig. 6c) because of complete etching. Similar strategies have been applied to prepare ZnO [40], Cu_2O [41], MnO [38] hollow structures. A schematic illustration of the hollow hematite microspheres formation process is presented in Fig. 7.

To further validate the formation mechanism of the hollow α-Fe_2O_3 microspheres by acetic acid etching, the results of FT-IR spectroscopy analysis and thermogravimetric analysis of the as-synthesized hollow α-Fe_2O_3 microspheres are shown in Figs. 8 and 9, respectively. The bands around 550 and 475 cm^{-1} are the characteristic absorption bands of the Fe–O of α-Fe_2O_3 [32], which confirms the hematite phase (Fig. 8). The two bands at 3435 and 1634 cm^{-1} are assigned to the O–H stretching and H–O–H bending modes of vibration, respectively, due

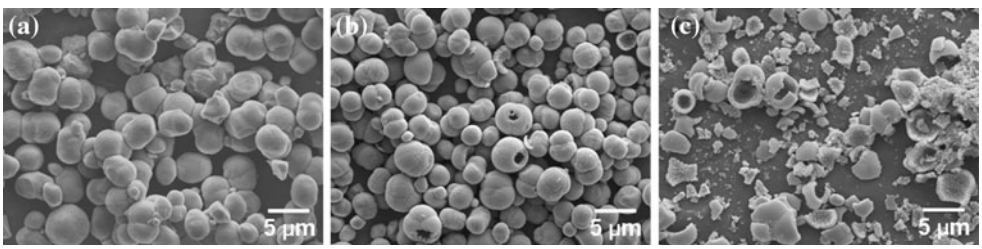

Fig. 6 SEM images of the hematite particles produced at 160 °C for 20 h under different the initial pH. **a** 1.4, **b** 1.1, **c** 0.7

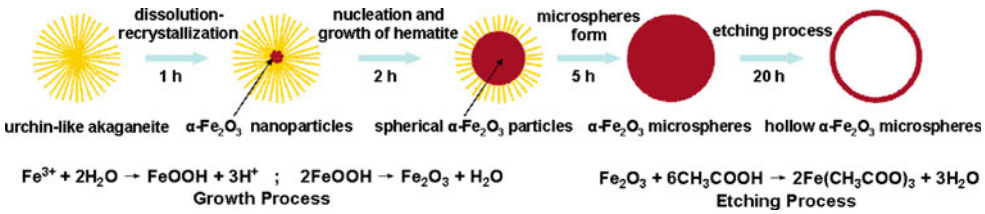

Fig. 7 A schematic illustration of the formation process of the hollow hematite microspheres

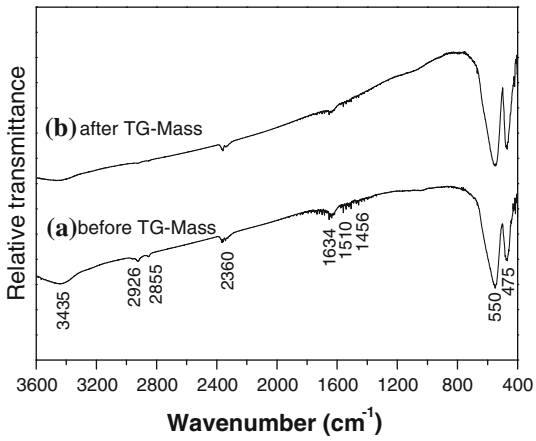

Fig. 8 The FT-IR spectrum of the hollow hematite microspheres produced at 160 °C for 20 h under the initial pH of 0.9. (*a*) Before TG-Mass, (*b*) after TG-Mass

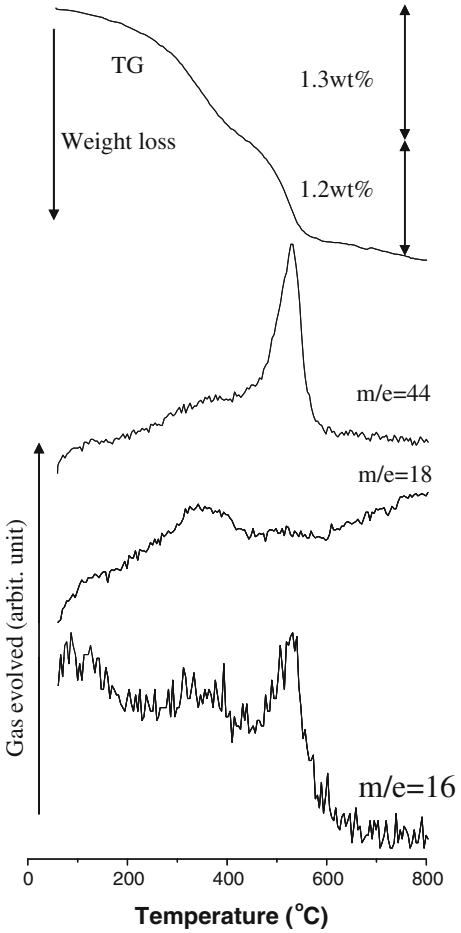

Fig. 9 TG curve and gas evolution during TG measurement of the hollow hematite microspheres produced at 160 °C for 20 h under the initial pH of 0.9

to H_2O absorbed in the product [32]. Corresponding to the results in Fig. 9, the first weight loss is at 400 °C, due to the release of H_2O molecules adsorbed on the surface of the hollow α-Fe_2O_3 microspheres. These H_2O molecules may have come from the acetic acid etching process. The band at 2360 cm^{-1} indicates the C–O vibration of CO_2 adsorbed on the particle surface (Fig. 8) [42]. The bands at 2855 and 2926 cm^{-1} are attributed to C–H vibrations [43, 44]. Two other strong absorptions at 1510 and 1456 cm^{-1} are due to symmetric and asymmetric stretching vibrations of the COO^- group of the acetate anion, showing the presence of the COO^- group in the products [45, 46]. These bands are ascribed to acetate (CH_3COO^-) derived from the acetic acid etching process, where acetate adsorbed on the surface or inside the hollow α-Fe_2O_3 microspheres. The weight loss at 600 °C is caused by the evolution of CH_4 and CO_2 gas (Fig. 9), with an m/e = 16 and 44, respectively. The weight loss is caused by the release of CH_4 and CO_2, resulting from the decomposition of acetate adsorbed on the surface or inside the hollow α-Fe_2O_3 microspheres. Moreover, in the FT-IR spectrum of the sample heated after TG-mass spectroscopy, the bands at 1456, 1510, 2855, and 2926 cm^{-1} disappears (Fig. 8b), which indicates that the acetate is completely decomposed during the TG-mass process. Thus, the hollow α-Fe_2O_3 microspheres formed probably originates from the acetic acid etching process.

Conclusions

Hollow hematite microspheres with an average diameter of 3–4 μm and a shell thickness of approximately 150 nm were synthesized under hydrothermal conditions using a $FeCl_3 \cdot 6H_2O$ solution and acetic acid without using a template. A possible formation mechanism for the hollow hematite microspheres was proposed based on time and the initial pH dependent experiments, which demonstrated that the acetic acid played a role in chemical etching. Changes in morphology with the reaction conditions, such as temperature and concentration of the $FeCl_3 \cdot 6H_2O$ solution,

were discussed. The as-synthesized hollow hematite microspheres may potentially be useful in water treatment, photocatalysis, and lithium ion batteries.

References

1. Lou XW, Archer LA, Yang ZC (2008) Adv Mater 20:3987
2. Caruso F, Caruso RA, Möhwald H (1998) Science 282:1111
3. Caruso F (2000) Chem Eur J 6:413
4. Caruso F (2001) Adv Mater 13:11
5. Schärtl W (2000) Adv Mater 12:1899
6. Zhong Z, Yin Y, Gates B, Yia Y (2000) Adv Mater 12:206
7. Fowler CE, Khushalani D, Mann S (2001) J Mater Chem 11:1968
8. Zhao WR, Chen HR, Li YS, Li L, Lang MD, Shi JL (2006) Adv Funct Mater 16:2243
9. Bertling J, Blömer J, Kümmel R (2004) Chem Eng Technol 27:829
10. Xiao LF, Zhao YQ, Yin J, Zhang LZ (2009) Chem Eur J 15:9442
11. Du N, Zhang H, Chen J, Sun J, Chen B, Yang D (2008) J Phys Chem B 112:14836
12. Liu GX, Hong GY (2005) J Solid State Chem 178:1647
13. Caruso RA, Susha A, Caruso F (2001) Chem Mater 13:400
14. Shen W, Zhu Y, Dong X, Gu J, Shi J (2005) Chem Lett 34:840
15. Wu ZC, Zhang M, Yu K, Zhang SD, Xie Y (2008) Chem Eur J 14:5346
16. Chen XY, Zhang ZJ, Li XX, Shi CW (2006) Chem Phys Lett 422:294
17. Chen T, Colver PJ, Bon SAF (2007) Adv Mater 19:2286
18. Zimmermann C, Feldmann C, Wanner M, Gerthsen D (2007) Small 3:1347
19. Zhang DB, Qi LM, Ma JM, Cheng HM (2002) Adv Mater 14:1499
20. Cornell RM, Schwertmann U (2003) The iron oxides: structure, properties, reactions, occurrences, uses. Wiley-VCH Verlag GmbH & Co. KGaA, Weinheim
21. Willard MA, Kuriharal LK, Carpenter EE, Calvin S, Harris VG (2004) Int Mater Rev 49:125
22. Huo L, Li W, Lu L, Cui H, Xi S, Wang J, Zhao B, Shen Y, Lu Z (2000) Chem Mater 12:790
23. Dong WT, Zhu CS (2002) J Mater Chem 12:1676
24. Kodama RH, Makholoufand SA, Berkowitz AE (1997) Phys Rev Lett 79:1393
25. Wu ZC, Yu K, Zhang SD, Xie Y (2008) J Phys Chem C 112:11307
26. Lian SY, Wang EB, Gao L, Wu D, Song YL, Xu L (2006) Mater Res Bull 41:1192
27. Li L, Chu Y, Liu Y, Dong L (2007) J Phys Chem C 111:2123
28. Cao SW, Zhu YJ (2008) J Phys Chem C 112:6253
29. Cao SW, Zhu YJ (2008) J Phys Chem C 112:12149
30. Zhang YP, Chu Y, Dong LH (2007) Nanotechnology 18:435608
31. Jagadeesan D, Mansoori U, Mandal P, Sundaresan A, Eswaramoorthy M (2008) Angew Chem Int Ed 47:7685
32. Dong Q, Wang D, Yao JX, Kumada N, Kinomura N, Takei T, Yonesaki Y, Cai Q (2009) J Ceram Soc Jpn 117:245
33. Dong Q, Kumada N, Yonesaki Y, Takei T, Kinomura N (2009) J Ceram Soc Jpn 117:881
34. Dong Q, Kumada N, Yonesaki Y, Takei T, Kinomura N (2010) J Ceram Soc Jpn 118:222
35. Lee JH (2009) Sens Actuators B 140:319
36. An K, Hyeon T (2009) Nano Today 4:359
37. Kuo TJ, Kuo CL, Kuo CH, Huang MH (2009) J Phys Chem C 113:3625
38. An K, Kwon SG, Park M, Na HB, Baik SI, Yu JH et al (2008) Nano Lett 8:4252
39. Chavez KL, Hess DW (2001) J Electrochem Soc 148:640
40. Zeng H, Cai W, Liu P, Xu X, Zhou H, Klingshirn C, Kalt H (2008) ACS Nano 2:1661
41. Kuo CH, Huang MH (2008) J Am Chem Soc 130:12815
42. Jing ZH, Wu SH, Zhang SM, Huang WP (2004) Mater Res Bull 39:2057
43. Pei ZF, Ponec V (1996) Appl Surf Sci 103:171
44. Kim JK, Oh HS, Jo CW, Suh YJ, Jang HD, Koo KK (2009) Chem Eng Res Des. doi:10.1016/j.cherd.2009.08.011
45. Zając EK, Marek KG, Datka (2006) J Microporous Mesoporous Mater 96:216
46. Hong RY, Fu HP, Di GQ, Zheng Y, Wei DG (2008) Mater Chem Phys 108:132